Direct Observation and Theory of Trajectory-Dependent Electronic Energy Losses in Medium-Energy Ion Scattering

A. Hentz,[1] G. S. Parkinson,[1,†] P. D. Quinn,[1,‡] M. A. Muñoz-Márquez,[1,§] D. P. Woodruff,[1,*] P. L. Grande,[2] G. Schiwietz,[3] P. Bailey,[4] and T. C. Q. Noakes[4]

[1]*Physics Department, University of Warwick, Coventry CV4 7AL, United Kingdom*
[2]*Universidade Federal do Rio Grande do Sul, Instituto de Fisica, Avenida Bento Gonçalves 9500, 91501-970 Porto Alegre, RS, Brazil*
[3]*Helmholtz-Zentrum Berlin f. Materialien u. Energie GmbH, Glienicker Strasse 100, 14109 Berlin, Germany*
[4]*STFC Daresbury Laboratory, Daresbury, Warrington WA4 4AD, United Kingdom*

(Received 8 December 2008; published 6 March 2009)

The energy spectrum associated with scattering of 100 keV H^+ ions from the outermost few atomic layers of Cu(111) in different scattering geometries provides direct evidence of trajectory-dependent electronic energy loss. Theoretical simulations, combining standard Monte Carlo calculations of the elastic scattering trajectories with coupled-channel calculations to describe inner-shell ionization and excitation as a function of impact parameter, reproduce the effects well and provide a means for far more complete analysis of medium-energy ion scattering data.

DOI: 10.1103/PhysRevLett.102.096103 PACS numbers: 68.49.Sf, 34.50.Bw, 79.20.Rf

Medium-energy ion scattering (MEIS) [1], typically using 100 keV incident H^+ or He^+ ions, is now an established technique for investigating the compositional and structural properties of the outermost few atomic layers of a solid. Like conventional (MeV) Rutherford backscattering (RBS), the combined effects of elastic recoil energy loss and inelastic losses allow one to determine the depth distribution of the near-surface composition. The combination of a high probability of electronic energy loss and high instrumental resolution, both associated with lower ion energies, means that MEIS can provide atomic-scale depth resolution. This is proving particularly valuable in the study of ultrathin films (such as those of high-κ dielectrics [2]), nanoclusters [3], and strained layers [4]. However, the full potential to exploit this has been constrained by an inadequate description of the electronic energy-loss process along the short scattering trajectory in the solid. Here, we present clear direct experimental evidence of the influence of trajectory-dependent inelastic energy loss in scattering from the outermost few atomic layers of a single crystal, and show that this can be modeled computationally in a parameter-free fashion.

If the ions travel through many atomic layers in the solid, as in RBS, data can be analyzed using an average energy loss per unit distance travelled by the ions in the sample, typically estimated using the SRIM code [5], which takes no account of the crystallographic character of the sample. Reduced rates of energy loss are known to occur in channelling along low index directions of crystals [6], and these are treated in a semiempirical fashion. At MEIS energies, electronic energy losses dominate, and the fact that these are impact-parameter dependent has been shown in studies of grazing-incidence ''skimming'' trajectories above a surface [7]. However, in MEIS studies of scattering from the outermost few atomic layers, it is important to recognize explicitly that the energy loss due to discrete electronic excitations, mainly of shallow core levels, depends on the exact trajectory of the ions relative to the atoms that they pass. The impact-parameter dependence of these electronic energy losses in single atom collisions can be described in a formulation based on *ab initio* quantum mechanical methods using full numerical atomic-orbital coupled-channel calculations [8], and we have recently shown that this approach leads to a good description of experimental data for scattering from isolated atoms adsorbed on surface [9]. Here, we show that, by incorporating this description of the energy loss into the well-established VEGAS program [10] to conduct a Monte Carlo calculation of the ion trajectories through the solid, we can correctly describe the inelastic energy loss involved in scattering from subsurface atoms in different experimental geometries. Previous treatment of this problem used either a heavily parameterized description of the energy-loss process [11], or the SILISH code [12] that provides a less accurate description of the scattered-ion trajectories away from blocking directions than VEGAS.

Clear evidence of the effect of trajectory-dependent energy loss in MEIS is provided by the experimental data of Fig. 1, which shows the intensity and peak width (variance) of the ''surface'' peak in the scattered-ion energy spectrum, resulting from 100 keV H^+ scattering from a clean Cu(111) surface, as a function of scattering angle. Using a $[\overline{411}]$ incident direction, only the outermost three atomic layers of the Cu(111) sample are fully illuminated (Fig. 2), as atoms in these three layers elastically shadow all deeper layers, except for a small amount of subsurface illumination due to atomic displacements arising from thermal vibration and surface relaxation. At a scattering angle of 109.5° in the $[\bar{2}11]$ azimuth, most of the scattered ions from Cu atoms in subsurface layers are prevented

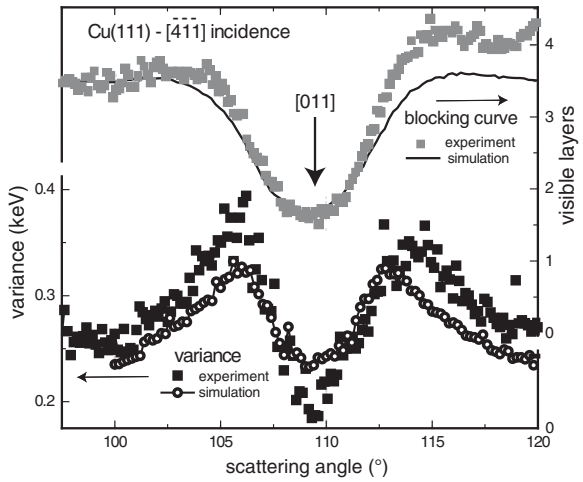

FIG. 1. Scattering-angle dependence of the scattered-ion intensity, and the width (variance) of the peak in the scattered-ion energy spectrum for $[\bar{4}\,\bar{1}\,\bar{1}]$ incidence of 100 keV H^+ ions. The blocking dip at 109.5° corresponds to emission along [011].

from reaching the detector by elastic scattering from Cu atoms in the higher layers, leading to a strong "blocking" dip along [110] in the scattered-ion intensity. The VEGAS program simulates this well (Fig. 1). This blocking dip coincides with a minimum in the variance of the scattering peak because at this angle, most of the detected ions are scattered only from the outermost Cu atoms and suffer electronic energy loss only in this single hard collision. For scattering angles a few degrees from the center of this blocking dip, the scattered-ion yield is enhanced; ions scattered from the second- and third-layer atoms can now reach the detector. These ions must pass close to Cu atoms in the uppermost layers, leading to a high probability of exciting electronic transitions in these atoms, enhanced energy loss, and an increased variance in the peak width. Scattering from these subsurface Cu atoms also contributes to the measured ion signal at angles further from the blocking dip, but these outgoing trajectories do not pass so closely to the outer layer Cu atoms, thus suffering less electronic energy loss; this leads to a reduced width of the scattered-ion energy peak. Notice that the angles of maximum peak width are slightly closer to the center of the blocking dip than the angles at which the maximum scattering yield is observed. The intensity maximum occurs at an angle at which all ions scattered from the second- and third-layer atoms can escape the surface without significant elastic scattering, but these outgoing trajectories do not pass so closely to the outer layer atoms, and so suffer less electronic energy loss.

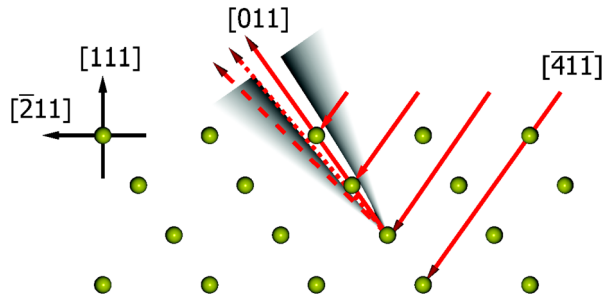

FIG. 2 (color online). Schematic diagram showing the incident and scattered-ion geometry from Cu(111) investigated in this work. The short-dashed and long-dashed lines show outgoing trajectories passing close ("skimming") and less close to atoms in the outermost surface layers (along the edge of the [011] shaded blocking cone).

The experiments providing the data of Fig. 1 were performed in an ultrahigh vacuum (UHV) end-station of the Daresbury Laboratory UK National MEIS facility [13] using 100 keV H^+ ions. These high-resolution MEIS measurements used a reduced vertical size of the ion beam of 0.15 mm, and were performed at room temperature with an ion dose of approximately 8×10^{15} ions/cm^2. Scattered ions were detected by a moveable toroidal electrostatic analyzer, the two-dimensional (2D) detector [14] of which provides "tiles" of ion counts as a function of both ion energy and scattering angle over limited ranges of each. The methodology for extracting ion energy spectra and angular blocking curves from these raw data tiles has been described elsewhere [13,15]. The data presented here are based on spectra summed over 10 channels of the detector (each corresponding to an angular range of ~0.15°) after correcting for energy shifts as a function of scattering angle. The Cu(111) crystal was cleaned *in situ* by cycles of ion bombardment and annealing to achieve a clean well-ordered surface as judged by Auger electron spectroscopy and low-energy electron diffraction (LEED).

In order to provide a theoretical description of our data, we have modified the standard VEGAS code, widely used to describe absolute scattering yields (in terms of the number of visible layers) and blocking curves in MEIS, to include the effects of trajectory-dependent energy loss. The key requirement to do this is a set of theoretical electronic energy-loss spectra as a function of impact parameter for the combination of Cu atom scatterers and 100 keV H^+ incident ions; this was obtained from the solution of the time-dependent Schrödinger equation for one active electron ("coupled-channel calculations") in the independent-electron model (IEM). Coupled-channel calculations are the best tool to describe inner-shell ionization and excitation of atoms [8,16] as a function of the impact parameter and are based on a semiclassical method [17]. The incident ion, following a classical trajectory, provides a time-dependent electrostatic perturbation on the target electrons which is incorporated into a full numerical solution of the time-dependent Schrödinger equation. For each impact parameter b, the amplitudes $a_{i\to f}$ are calculated for any transition from an initial occupied state i to an unoccupied bound or continuum state f, giving the probability of atomic excitation or ionization. These calculations yield

the energy loss or energy transfer (T) probability, dP/dT, for each atomic subshell as a function of b, including a nonzero probability for no-loss collisions; for $T > 0$, dP/dT is continuous apart from some spikes due to excitations to bound states. Previous reports provide fuller details of the atomic-orbital coupled-channel calculations (AO) [8], and their application to the MEIS technique in particular [9]. The VEGAS code was modified to assign an energy loss to each close encounter of the incident and scattered ions with an atom in the solid as they pass though the outermost atomic layers; each energy loss was selected by a random number generator from the dP/dT function calculated for the appropriate impact parameter. The final energy-loss spectrum associated with the emerging ions was then convoluted with a Gaussian instrument function [9] for comparison with the experimental data. The asymmetry of the scattered-ion energy spectra thus arises entirely from the electronic energy losses.

The good fit seen in Fig. 1 of the experimental and simulated blocking curves—the variation of the scattered-ion yield, expressed in terms of the number of contributing (''visible'') atomic layers, as a function of scattering angle—is a well-known feature of the VEGAS code. However, the generally good match to the experimentally observed variation in the peak width, due to trajectory-dependent energy loss, is a unique feature of our modified code. Figure 3 shows a comparison of the scattered-ion energy spectra at several scattering angles within the range covered by Fig. 1. In Fig. 3, the peak intensities have been normalized to a constant value, and the energies have been displaced by the (scattering-angle dependent) kinematical recoil energy loss to allow clearer comparison of the peak shapes. The quantitative agreement is not perfect at the bottom of the blocking dip, but in all other respects, the agreement is excellent.

One interesting feature of Fig. 3 is not only the variation of the peak shape but also a displacement of the peak energy resulting from the different trajectory-dependent energy losses. This shift in peak energy is to be expected; for scattering geometries displaced in angle from the blocking dip, new scattered intensity appears, mainly from second- and third-layer scattering events, and these contributions are displaced to lower energy due to the increased electronic energy loss of these ions with longer trajectories in the solid. This same effect contributes to the increased peak width. However, as the displacement of the scattering angle from the blocking dip increases, the peak narrows, but the peak position shifts very little. This is because the relative importance of higher-energy electronic energy loss is much greater for the ''skimming'' exit trajectories close to the blocking geometry. Significant ionization of deeper core levels in the atoms of the solid and production of faster electrons is only achieved at relatively small impact parameters and, apart from in the single ''hard'' (large scattering-angle) collision

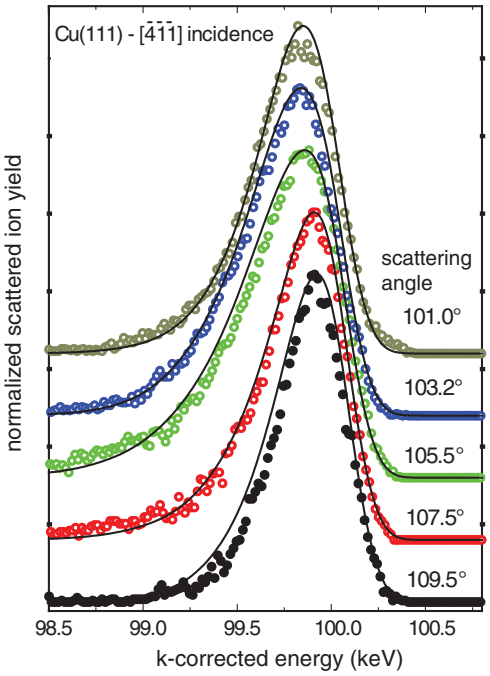

FIG. 3 (color online). Comparison of the experimental (circles) and theoretical (full line) scattered-ion energy spectra for [$\bar{4}\,\bar{1}\,\bar{1}$] incidence of 100 keV H^+ ions on a Cu(111) surface at different scattering angles in the [$\bar{2}11$] azimuth. The [011] blocking direction is at 109.5°. Energies have been offset by the kinematic elastic recoil energy, and peak intensities are normalized to the same value to aid comparison of peak shapes and relative energies.

suffered by all the detected ions, these can only occur for trajectories in which the ions pass very close to atoms on their outward trajectory.

This combined description of both elastic and inelastic scattering in MEIS allows us to model the complete two-dimensional map of ion counts as a function of ion energy and scattering angle provided by the experimental instrumentation. Figure 4 shows such a comparison of experimental and simulated data for scattering in this same angular range around the [011] emission direction, also using [$\overline{411}$] incidence of 100 keV H^+ ions, the scattered-ion intensity being represented by different colors. The simulation clearly shows all the main features of the experimental data, notably the Cu ''surface'' scattering peak (the high-intensity diagonal line from the top left towards the lower right-hand side of the map), and the [011] blocking dip which appears as a vertical line of reduced intensity around a scattering angle of 109.5°. The main difference between the two maps is the nonzero scattering intensity at low energies in the experimental data, associated with dechannelling deep in the substrate, an effect not included in the calculations of scattering from the outermost nine atomic layers of the surface. Figure 4 clearly shows that it is the increased intensity and extent of the low-energy ''tail'' of the scattered-ion energy spectrum that is the

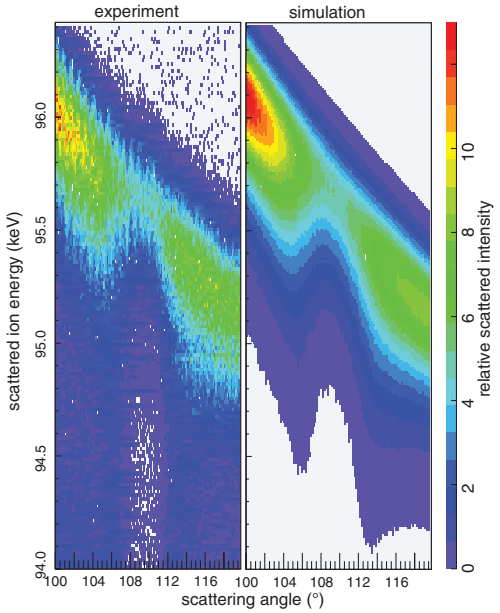

FIG. 4 (color online). Two-dimensional map of scattered-ion intensities as a function of scattering-angle and scattered-ion energy around the [011] blocking dip (at 109.5°) for $[\bar{4}\,\bar{1}\,\bar{1}]$ incidence of 100 keV H^+ ions on Cu(111). The raw experimental data are compared with the theoretical simulation.

strongest signature to the trajectory-dependent electronic energy loss. The strong modulation in the energy of the low-energy edge of the contour map is a direct manifestation of this, and reflects the angular variation of the peak width shown in Fig. 1.

In summary, our experimental measurements of the scattered-ion yield and the scattered-ion energy-loss spectra for 100 keV H^+ scattering from Cu(111) as a function of scattering geometry provide a particularly clear illustration of the role of trajectory-dependent energy loss in MEIS. Moreover, we show that a modified version of the VEGAS simulation code that explicitly includes the role of trajectory-dependent electronic energy loss, in a parameter-free fashion, provides an excellent description of these phenomena. The ability to describe both of these aspects of experimental MEIS data offers a means of significantly increasing the information that can be extracted from such experiments in terms of the atomic-scale depth dependence of the composition and structure. The approach here, using *ab initio* calculations of the impact-parameter dependence of the energy loss in single collisions, is computationally very demanding, but recent work indicates that a simple analytic form provides a good approximation for this purpose [18], and, indeed, that it has already been shown to be effective in describing MEIS from noncrystalline samples in which the trajectory dependence is not an issue [19].

The authors acknowledge funding support by the Engineering and Physical Sciences Research Council (UK), by CNPq, and CAPES (Brazil).

*Corresponding author: d.p.woodruff@warwick.ac.uk
†Department of Physics, Tulane University, New Orleans, Louisiana 70118, USA
‡Diamond Light Source, Harwell Science and Innovation Campus, Didcot, OX11 0DE, UK
§Instituto de Ciencia de Materiales de Sevilla (CSIC-US), Americo Vespucio 49, 41092 Sevilla, Spain

[1] J. F. van der Veen, Surf. Sci. Rep. **5**, 199 (1985).
[2] M. Copel, Appl. Phys. Lett. **92**, 152909 (2008).
[3] A. Iwamoto *et al.*, Nucl. Instrum. Methods Phys. Res., Sect. B **266**, 965 (2008).
[4] S.-J. Kahng *et al.*, Phys. Rev. Lett. **80**, 4931 (1998).
[5] J. F. Ziegler, SRIM code, http://www.SRIM.org.
[6] D. S. Gemmel, Rev. Mod. Phys. **46**, 129 (1974).
[7] S. Lederer and H. Winter, Phys. Rev. A **73**, 054901 (2006).
[8] G. Schiwietz, Phys. Rev. A **42**, 296 (1990); P. L. Grande and G. Schiwietz, Phys. Rev. A **44**, 2984 (1991); G. Schiwietz and P. L. Grande, Nucl. Instrum. Methods Phys. Res., Sect. B **69**, 10 (1992); P. L. Grande and G. Schiwietz, Phys. Rev. A **47**, 1119 (1993).
[9] A. Hentz *et al.*, Phys. Rev. B **74**, 125408 (2006).
[10] J. W. M. Frenken, R. M. Tromp, and J. F. vander Veen, Nucl. Instrum. Methods Phys. Res., Sect. B **17**, 334 (1986).
[11] P. F. A. Alkemade, W. C. Turkenburg, and W. F. van der Weg, Nucl. Instrum. Methods Phys. Res., Sect. B **28**, 161 (1987).
[12] P. L. Grande *et al.*, Phys. Rev. B **69**, 104112 (2004).
[13] P. Bailey, T. C. Q. Noakes, and D. P. Woodruff, Surf. Sci. **426**, 358 (1999).
[14] R. M. Tromp *et al.*, Rev. Sci. Instrum. **62**, 2679 (1991).
[15] D. Brown *et al.*, J. Phys. Condens. Matter **11**, 1889 (1999).
[16] W. Fritsch and C. D. Lin, Phys. Rep. **202**, 1 (1991); J. F. Reading *et al.*, J. Phys. B **30**, L189 (1997).
[17] J. Bang and J. M. Hansteen, K. Dan. Vidensk. Selsk. Mat. Fys. Medd. **31**, 13 (1959); L. Wilets and S. J. Wallace, Phys. Rev. **169**, 84 (1968); M. R. Flannery and K. J. MacCann, Phys. Rev. A **8**, 2915 (1973).
[18] P. L. Grande *et al.*, Nucl. Instrum. Methods Phys. Res., Sect. B **256**, 92 (2007).
[19] R. P. Pezzi *et al.*, Appl. Phys. Lett. **92**, 164102 (2008).